

# Overpredictive Signal Analytics in Federated Learning: Algorithms and Analysis

Vijay Anavangot

*Department of Electrical Engineering,  
Indian Institute of Technology Bombay,  
Mumbai - 400076, India  
Email: a.vijay.2014@ieee.org*

---

## Abstract

Edge signal processing facilitates distributed learning and inference in the client-server model proposed in federated learning. In traditional machine learning, clients (IoT devices) that acquire raw signal samples can aid a data center (server) learn a global signal model by pooling these distributed samples at a third-party location. Despite the promising capabilities of IoTs, these distributed deployments often face the challenge of sensitive private data and communication rate constraints. This necessitates a learning approach that communicates a processed approximation of the distributed samples instead of the raw signals. Such a decentralized learning approach using signal approximations will be termed distributed signal analytics in this work. Overpredictive signal approximations may be desired for distributed signal analytics, especially in network demand (capacity) planning applications motivated by federated learning. In this work, we propose algorithms that compute an overpredictive signal approximation at the client devices using an efficient convex optimization framework. Tradeoffs between communication cost, sampling rate, and the signal approximation error are quantified using mathematical analysis. We also show the performance of the proposed distributed algorithms on a publicly available residential energy consumption dataset.

*Keywords:* Distributed Algorithms, Statistical Learning, Optimization, Approximation methods, Signal Analysis

---

## 1. Introduction

Distributed signal (or information) processing using Internet of Things (IoT), facilitates real time monitoring of signals (such as environmental pollutants, financial, energy consumption) in a smart city. Despite promising capabilities, these distributed deployments often face the challenge of data privacy and communication rate constraints [1, 2]. In traditional machine learning, training data is moved to a data center, which requires massive data movement from distributed IoT devices to a third-party location, thus raising concerns over privacy and ineffi-

cient use of communication resources. Moreover, the growing network size, model size, and data volume combined lead to unusual complexity in the design of optimization algorithms, beyond the compute capability of a single device. This necessitates novel system architectures to ensure stable and secure operations. Federated learning (FL) architecture can be a promising solution for enabling IoT-based smart city applications, by addressing these challenges [3, 4, 2, 5, 6, 7]. In the FL paradigm, a global server orchestrates model training, without raw-data being transferred from the participating devices (or clients). Edge-deployed signal processing algorithms, such as sparse approximations and statistical learning methods will be essential for efficient management of compute and communication resources in FL.

In certain networked system applications, such as electricity network demand planning, or flood/drought forecasting systems or Unmanned Aerial Vehicle (UAV) path planning, or autonomous driving it is essential to have an overpredictive estimate of signals. For instance, consider a smart city application shown in Fig. 1, where each household has a smart energy meter to monitor and record the instantaneous electric power. At the end of the day, each smart meter will need to report an approximate summary of the consumer side energy usage to a centrally located server, accessible to the electricity network planner. The planner desires to have an overpredictive estimate of the energy demand time-series, so that the generation can be planned to always meet the consumer demand. In such a smart city application, we attempt to answer the question, *how to perform overpredictive signal analytics when the devices are distributed?*. The significant challenges in doing such distributed signal analytics in FL are identified to be: (1) asymmetric communication resources (i.e. uplink rate is less than the downlink rate), (2) heterogeneous devices, (3) sensitive private data, and (4) scale of operation (a large number of devices) [2]. This work will primarily address communication rate constraints while implicitly ensuring user privacy and scalability. In this first exposition, we restrict the focus to the class of homogeneous user devices. FL allows a common global model to be learned from distributed devices by using efficient compressed signal representations. The existing literature in FL, however, has a focus on learning a parametric model using a central parametric server, such as a neural network model through the successive exchange of gradients [3, 4, 2, 5, 8, 9]. In this work, the approach is different as we utilize the FL architecture for learning signal analytics [10], instead of a parametric model. The goal is to achieve efficient statistical representation for performing analytics involving signal overprediction.

A key feature in FL is to utilize edge signal processing to perform distributed signal analytics. Let us revisit the example of energy demand time-series aggregation performed at the smart city electricity server, as illustrated in Fig. 1. This central server performs network planning

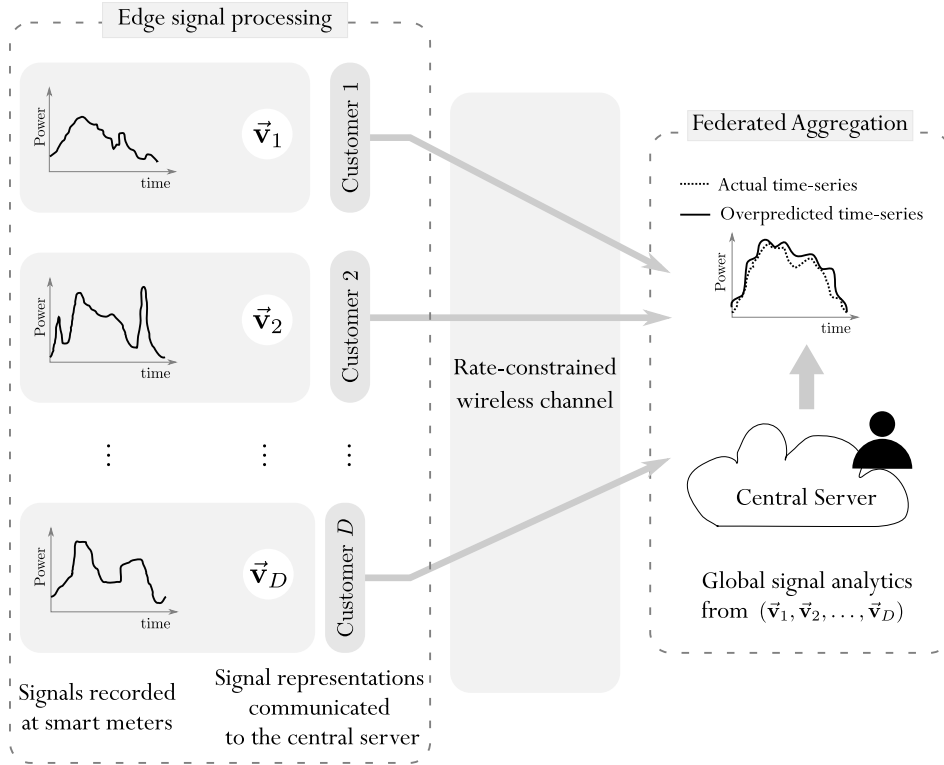


Figure 1: The figure illustrates federated learning for overpredictive signal analytics in a smart city with  $D$  electricity consumers. The power consumption time-series recorded at the consumer’s smart meters are converted to compressed signal representations,  $\{\vec{v}_1, \vec{v}_2, \dots, \vec{v}_D\}$  using edge signal processing. These signal representations are communicated to the central server for computing signal analytics that overpredict the actual demand time-series.

to meet the electricity demands of the consumers in the city. At each of the  $D$  consumers (also known as edge/client devices), the installed smart meter would record the instantaneous power consumed and communicate a compressed representation, *viz.*  $\{\vec{v}_1, \vec{v}_2, \dots, \vec{v}_D\}$ , of the demand signal to the server through a rate-constrained wireless channel. The network planner aggregates the client signal representations to estimate an approximate demand time-series signal, which over-predicts the actual aggregate demand signal. A possible implementation scheme would be to compute approximate signal representations locally at the edge devices such that these representations satisfy the individual signal overprediction constraints. The edge devices then communicate these compressed signal representations to the server, where signal analytics of interest are computed. The signal analytics desired at the server may include the peak electric power demand or the aggregate signal Cumulative Distribution Function (CDF). Such overpredicted demand signal analytics computed from the approximate signal representations  $\{\vec{v}_1, \vec{v}_2, \dots, \vec{v}_D\}$ , will reduce the client-server communication cost. Since the actual data does not move to the server, implicit data privacy is achieved. The computed signal analytics at the server is useful to maintain the stability and security of the electricity distribution network.

Our main contributions in this work are summarized below.

- We consider signal approximation based on overprediction constraint in the federated learning setup by using the Fourier basis for signal representation.
- We develop a aggregation procedure at the central server to learn the global signal analytics, by relying on the empirical CDF of the aggregate signal.
- We derive mathematical upperbounds on the pointwise difference of the actual signal CDF and the Glivenko-Cantelli CDF estimate of the overpredicted signal, considering the effect of signal sampling.
- We present the tradeoff between the communication cost and the signal approximation error, and validate it using experiments on a publically available residential energy consumption dataset [11].

### 1.1. Prior Literature

Using the federated learning (FL) approach, communication-efficient distributed learning was introduced by McMahan et al. [2]. The FL architecture proposed in this work considers massively distributed, heterogeneous devices, which have limited communication. The authors illustrate the utility of FL models for training deep neural networks with on-device data using stochastic gradient descent (SGD) based *FedAvg* algorithm. An improved *FedProx* algorithm was later proposed to handle system heterogeneity in FL, which in addition has convergence guarantees [12]. In another related work, Suresh et al. [8] discuss a communication-efficient distributed mean estimation using FL, stochastic quantization, and structured rotation. Bonawitz et al. [5], has described the system-level implementation of FL algorithms in large-scale networks. Advances in FL algorithms, including open directions in distributed learning with privacy sensitive data, have been summarized in the review paper by Kairouz and McMahan [6]. From a signal processing perspective, the applications and challenges of FL have been discussed by Li et al. [7]. Signal processing methods such as compressed gradients and sketched updates have found utility in training and deploying FL in low-power TinyML devices [13, 14]. Further, FL models to address the fairness of resource allocation have been studied from the perspective of parametrized cost functions and empirical probability distributions [15, 16]. The references above mostly deal with single task FL models. Considering real-world IoT systems, a multi-task learning scheme was proposed [17] that allows for a certain degree of model personalization.

Several applications of signal overprediction are discussed in the literature. These include watershed management (hydrology), Unmanned Aerial Vehicle (UAV) path planning, CPU

power prediction, and database management for TV whitespace protection contours. In hydrology, flood and drought predictions are made possible through statistical learning approaches that use custom loss functions to include overprediction constraints [18]. Support Vector Machine (SVM) models utilizing asymmetric loss functions are generally used for CPU power cycle prediction [19]. Recent research shows that neural networks do not capture accurate depth information in images, which can have significant safety implications in autonomous driving [20]. Overpredicting ADC design is a suggested solution to overcome this safety challenge. Maheshwari and Kumar have proposed a novel quantizer design for the TV whitespace (geo-database management) application, which determines an overpredicting envelope [21]. In a recent research, a Federated learning (FL) approach considering personalized client attributes is analyzed for energy demand prediction using a clustered aggregation scheme [22]. In another related work, Konstantinos et al. studies the time-series dimensionality reduction approach with symbolic aggregate approximation (SAX) and Lloyd’s algorithm [23], using a combination of quantization and event-based sampling to achieve signal compression. Recently, Saputra et al. have examined the utility of FL algorithms for location-specific demand prediction in an electric vehicle (EV) charging architecture [24].

## 2. Distributed Signal Model and Background Concepts

In this section we describe the basic signal model using the FL architecture and discuss the related background concepts for overpredictive signal analytics. The signal model has been adapted from the abridged paper by Anavangot and Kumar [25].

### 2.1. Federated Learning Signal Model

We consider the federated learning architecture that consists of  $D$  distributed client devices and a centrally located server as shown in Fig. 2. Each client device in this model observes a continuous time signal  $f_i(t)$  for  $i \in \{1, 2, \dots, D\}$ . Without loss of generality we will assume that each observed signal has a bounded support in the time interval  $[0, 1]$ . Further, in the ensuing analysis, we also assume that these signals are  $p$ -times differentiable, such that  $p \geq 1$ . Under these signal assumptions, we devise algorithms to learn a global signal model using clients-server communication. Due to rate constrained nature of the client-server communication channel, the devices may communicate only an approximate signal, which we denote by  $\hat{f}_i(t)$  for  $i \in \{1, 2, \dots, D\}$ .

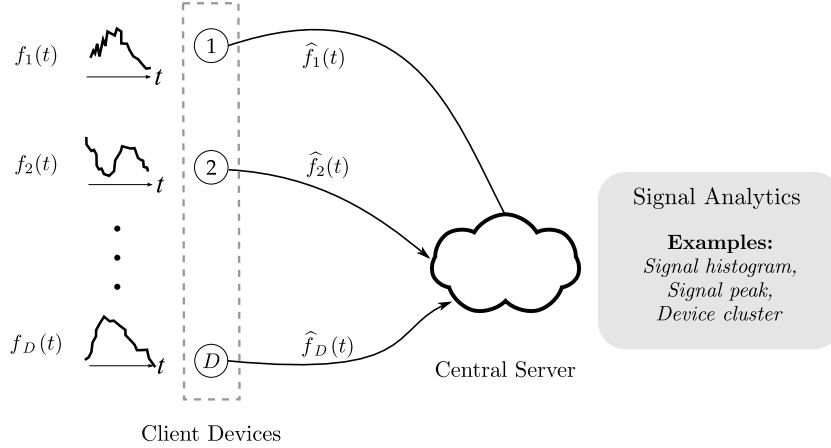


Figure 2: The system overview of a federated learning model adapted from [25]. In this model, the  $D$  participating client devices communicate an approximation of the observed signal, and the central server aggregates these signal approximations to learn global signal statistics such as histogram, signal peak, and device clusters.

## 2.2. Signal Representation

In this exposition, we represent the signals using the Fourier basis. That is, each recorded signal at the clients can be represented by a Fourier series,

$$f_i(t) = \sum_{k=-\infty}^{\infty} a_i[k] \exp(j2\pi kt), \quad t \in [0, 1],$$

where  $i \in \{1, 2, \dots, D\}$ . As the Fourier series representation is periodic we will assume  $f_i(0) = f_i(1)$ . From the  $p$ -times differentiability assumption, we observe a polynomial decay of Fourier series coefficients of the signal, which is stated in the fact below:

**Fact 1** (Sec 2.3,[26]). *A signal  $f(t), t \in [0, 1]$ , with  $f(0) = f(1)$ , is  $p$ -times differentiable if its Fourier coefficient  $a[k]$  satisfies the condition,*

$$|a[k]| \leq \frac{C}{|k|^{p+1+\varepsilon}} \quad \text{for some } C, p, \varepsilon > 0.$$

## 2.3. Problem Formulation and Related Definitions

For this signal approximation, consider the  $2L + 1$  length bandlimited approximation of the signals,  $f_i(t)$  for  $i \in \{1, 2, \dots, D\}$ , given by the Fourier series,

$$\hat{f}_i(t) = \sum_{k=-L}^L b_i[k] \exp(j2\pi kt) \quad \text{for } t \in [0, 1], \quad (1)$$

where the Fourier coefficients  $b_i[k]$  for  $k \in \{-L, \dots, L\}$ , will be a function of  $a_i[k], k \in \mathbb{Z}$ .

The approximation coefficients  $b_i[k]$  are computed by solving a constrained optimization program that minimizes the approximation error with respect to a distance metric  $d(\cdot)$ . Typical

distance metrics include  $\mathcal{L}_1$ ,  $\mathcal{L}_2$  or  $\mathcal{L}_\infty$  norm, subject to the overprediction constraint. The optimization can be stated as,

$$\arg \min_{\widehat{f}_i(t)} d(f_i(t), \widehat{f}_i(t)) \quad \text{subject to } \widehat{f}_i(t) \geq f_i(t). \quad (2)$$

Because the Fourier basis is orthogonal, an equivalent optimization problem can be framed in terms of the Fourier coefficients  $a_i[k]$ 's and  $b_i[k]$ 's. Therefore, when the distance metric is the  $\mathcal{L}_2$  norm, the equivalent optimization problem is

$$\arg \min_{b_i[k]} \sum_{k=-L}^L |a_i[k] - b_i[k]|^2 \quad \text{subject to } \widehat{f}_i(t) \geq f_i(t). \quad (3)$$

The considered problem has linear constraints that meet the overprediction criteria, hence the signal approximation obtained by this method will be called the *envelope approximation*. Throughout this paper we will denote the envelope approximation of a signal  $f(t)$  by  $\widehat{f}_{\text{env}}(t)$ .

#### 2.4. Choice of the distance metric

The choice of the distance metrics used to construct the envelope approximation from the signals recorded at each client device is described. Note that the envelope approximation  $\widehat{f}_{\text{env}}(t)$  of the signal  $f(t)$  is the solution to the optimization problem described in (2), with respect to a distance metric  $d(\cdot)$  defined over the signal space. In this paper, we restrict the analysis to the convex distance measures  $\mathcal{L}_1$  and  $\mathcal{L}_2$ , and later take up the  $\mathcal{L}_\infty$  formulation to derive performance bounds. By using the Fourier representation of  $\widehat{f}_{\text{env}}(t)$  (akin to (1), but with the subscript indices dropped) and  $f(t)$ , and the envelope property  $\widehat{f}_{\text{env}}(t) \geq f(t)$  it can be seen that,

$$\|\widehat{f}_{\text{env}} - f\|_1 = b[0] - a[0], \quad (4)$$

$$\|\widehat{f}_{\text{env}} - f\|_2^2 = \sum_{|k| \leq L} |b[k] - a[k]|^2 + \sum_{|k| > L} |a[k]|^2 \quad (5)$$

$$\|\widehat{f}_{\text{env}} - f\|_\infty \leq \sum_{|k| \leq L} |b[k] - a[k]| + \sum_{|k| > L} |a[k]| \quad (6)$$

For notational convenience, the signal approximation error corresponding to  $\mathcal{L}_1$ ,  $\mathcal{L}_2$  and  $\mathcal{L}_\infty$  distance measures will be denoted by  $\text{SA}_1$ ,  $\text{SA}_2$  and  $\text{SA}_\infty$  respectively. The upperbound in (6) will be used to show the performance bounds of envelope approximations in Section 4.1.

### 3. Algorithms for Overpredictive Signal Analytics

In this section, we describe the algorithms to execute envelope signal analytics using the federated learning model as illustrated in Fig. 2. For the distributed model with  $D$  devices, each

client device will report an overpredictive envelope approximation of the signal observed. These signal approximations are solutions to optimization programs implemented at the individual client devices. The envelope signals obtained are later aggregated to compute signal analytics at the central server. The algorithms presented here is an elaborated version of the the discussions in Anavangot and Kumar [25].

### 3.1. Algorithms at the Clients

The goal of the client devices is to compute the best possible envelope signal which approximates the true signal. The optimization problem of interest can be stated as,

$$\min \text{SA}_q := \int_0^1 |\hat{f}(t) - f(t)|^q dt \text{ subject to } \hat{f}(t) \geq f(t) \quad (7)$$

for  $q = 1, 2$ , where the above minimizations are over the individual approximate signals  $\hat{f}_1(t), \dots, \hat{f}_D(t)$ . These optimization problems can be efficiently solved using the equivalent Fourier domain representation and the respective norms, described in (4) and (5).

We note that the inequality constraints of the problem are linear. Thus, for  $q = 1$ , the above envelope approximation formulation will become a *linear program*, since the cost function in the Fourier representation is the difference of the zero frequency components of the envelope and true signal. When  $q = 2$  the problem is equivalent to a *quadratic program with linear constraints*, with the objective described by the squared error of the Fourier coefficients within bandwidth  $L$ . Both  $q = 1$  and  $q = 2$ , has linear inequality constraints due to the envelope overprediction criteria. The choice of the optimization problem to solve –  $\mathcal{L}_1$  or  $\mathcal{L}_2$ , depends on the tradeoff between mean squared error, subsampling and envelope violations. As linear programs have lower computational complexity when compared to quadratic programs, the client devices with limited hardware can choose to solve  $\mathcal{L}_1$  optimization problem over the  $\mathcal{L}_2$  problem.

#### *Envelope Optimization with Discrete-time Signals*

In practice, the recorded client device signals are available at  $n$  discrete time samples. Since the true signal values are unknown at all times except the sampled points, the set of inequality constraints in discrete-time case is a finite subset of the envelope constraints in the continuous time case. Hence, the discrete-time optimization yields a lower cost than the continuous-time optimization. A related analysis of the discrete-time envelope optimization in the context of TV whitespace application, along with Mean Squared Error (MSE) performance is discussed in [27]. More detailed analysis of the discrete time envelope optimization is presented in Sec 4.

### 3.2. Aggregation at the server

The signal analytic of interest is computed at the server by combining signal approximations reported at the edge devices. A signal analytic, in general, is a function over the envelope approximations  $\widehat{f}_i(t)$  for  $i \in \{1, 2, \dots, D\}$ . In this work we consider two examples of such signal analytics which include

1. the aggregate function,

$$\widehat{s}(t) := \sum_i \widehat{f}_i(t), \quad (8)$$

2. the Glivenko-Cantelli empirical CDF,

$$\widehat{F}_N(x) := \frac{1}{N} \sum_{n=1}^N \mathbb{1}_{(-\infty, x]}(\widehat{f}(t_n)), \quad (9)$$

where  $\mathbb{1}_{(-\infty, x]}(Y)$  represents the 0–1 indicator function for the probability event  $\{Y \leq x\}$ , and  $t_n$  for  $n \in \{1, 2, \dots, N\}$  represents the time samples in the time interval  $[0, 1]$ .

This classical Glivenko-Cantelli estimate of the CDF [28], serves as a means to infer several statistical properties. Due to the uniform convergence property of the Glivenko-Cantelli estimate, at the server there exists an implicit minimization of an empirical loss function involving the actual and estimated CDFs, i.e. the objective function,

$$\|\widehat{F}_N(x) - F(x)\|_\infty, \quad (10)$$

is minimized by when  $\widehat{F}_N(x)$  is the Glivenko-Cantelli estimate of  $F(x)$ . This minimization task is in agreement with the definition of federated optimization [2]. We discuss further applications of CDF estimation based signal analytics in the section 5.

### 3.3. Federated learning algorithm for over-predictive signal analytics

We consider the FL model where client devices work in a distributed manner. It is assumed the each device has the hardware capability to compute the envelope signal with the constraint,  $\widehat{f}_i(t) \geq f_i(t)$  for  $i \in \{1, 2, \dots, D\}$ . The following algorithm is proposed to obtain a bandwidth- $L$  envelope approximation  $\widehat{f}_i(t)$  and later aggregated to derive a global signal analytic,  $G_{\text{server}}(\widehat{f}_1(t), \dots, \widehat{f}_D(t))$ .

In summary, the client step and the server step of the algorithm can be explained as:

1. From the signal  $f_i(t)$  recorded at device  $i$ , compute its envelope approximation  $\widehat{f}_{i,\text{env}}(t)$ , using the envelope optimization (7), and communicate the  $(2L + 1)$  Fourier coefficients to the server.

---

**Algorithm 1** Federated learning algorithm for overpredictive signal analytics

---

**Input:** Recorded signals  $f_i(t)$  at individual devices  $i \in \{1, 2, \dots, D\}$ .

**Initialize:** Fourier coefficients  $a_i[n]$  for  $n \in \{-L, \dots, 0, \dots, L\}$

**for**  $i \in \{1, 2, \dots, D\}$  **do**

- Compute  $\widehat{f}_{i,\text{env}}(t)$ , and coefficients  $b_i[n]$  for  $n \in \{-L, \dots, 0, \dots, L\}$  such that  $\widehat{f}_{i,\text{env}}(t) \geq f_i(t)$ .
- Communicate  $b_i[n]$  to the server

**end for**

**Return** global model computed  $G_{\text{server}}(\widehat{f}_{1,\text{env}}, \widehat{f}_{2,\text{env}}, \dots, \widehat{f}_{D,\text{env}})$  (for example, (8) or (9))

---

2. At the server the Fourier coefficients received from each client device are aggregated, to calculate a global model (or statistic) of interest, denoted as  $G_{\text{server}}(\widehat{f}_{1,\text{env}}, \widehat{f}_{2,\text{env}}, \dots, \widehat{f}_{D,\text{env}})$ .

Step 1 of the algorithm executed at the client devices is outlined next. For  $\mathcal{L}_1$  distance (see (4)), the optimization program becomes,

$$\begin{aligned} & \text{minimize } b[0] - a[0] \\ & \text{subject to } \vec{b}^T \Phi(t) \geq f(t), \end{aligned} \quad (11)$$

where  $\Phi(t) = [\exp(-2\pi Lt), \dots, \exp(2\pi Lt)]^T$  and  $\vec{b} = (b[-L], \dots, b[L])^T$  are the Fourier series coefficients of the envelope approximation. It is known that the above linear program with linear constraints is solvable efficiently [27]. For  $\mathcal{L}_2$  case, the cost function  $b[0] - a[0]$  is replaced by the quadratic cost in (5).

We understand that, as approximation bandwidth  $L$  is increased, the envelope signal  $\widehat{f}_{i,\text{env}}(t)$  become more proximal to their target signal  $f_i(t)$ . It is expected that the approximation errors,  $\text{SA}_1$  and  $\text{SA}_2$  will decrease as  $L$  increases. However, analyzing the dependence of  $\text{SA}_q$ ,  $q = 1, 2$  versus  $L$  is difficult. Accordingly, we rely on a naïve envelope approximation to analyze the fundamental bounds on their tradeoff.

#### 4. Performance Bounds on Optimal Envelope Approximation

In this section, we analyze the performance of the  $L$  bandwidth envelope approximation. In particular, we provide an upper bound for the envelope approximation error, using the idea of naïve envelope approximation scheme, described below.

##### 4.1. A Naïve Envelope Approximation Scheme

Let us consider a single client device,  $i = 1$  in isolation. Let  $f_{1,\text{proj}}(t)$  be the orthogonal projection of  $f_1(t)$  on the span of  $\exp(j2\pi kt)$  for  $|k| \leq L$ . Then  $f_{1,\text{proj}}(t) = \sum_{|k| \leq L} a_1[k] \exp(j2\pi kt)$ .

The naïve envelope approximation scheme is as follows [21]:

$$f_{1,\text{env}}(t) = f_{1,\text{proj}}(t) + C_0, \quad (12)$$

where  $C_0 = \|f_1 - f_{1,\text{proj}}\|_\infty$ . Using the triangle inequality,

$$C_0 \leq \sum_{|k|>L} |a_1[k]| \leq \sum_{|k|>L} \frac{C}{|k|^p}, \quad p > 1. \quad (13)$$

For  $p > 1$  [29, Sec. 2.2], we can show that,  $C_0 = O\left(\frac{1}{L^{p-1}}\right)$ .

#### 4.2. Envelope Approximation Analysis

In this section we seek the answer to the question – *Is there a class of signals for which the naïve envelope approximation is a good scheme?* The goodness here can be measured using the mean squared error. The result discussed below shows that there exist a certain class of signals for which the naïve approximation is order optimal to the optimal envelope scheme, while using  $\mathcal{L}_1$  or  $\mathcal{L}_2$  norm minimization.

In the result stated below we use the notation  $SA_q$  to denote the optimal envelope approximation error (see (4)), and the notation  $SA'_q$  to be the approximation error corresponding to the naïve envelope approximation in (12), where  $q \in \{1, 2\}$  according to the  $\mathcal{L}_1$  or  $\mathcal{L}_2$  cost metric.

**Theorem 1.** *The approximation errors of the optimal envelope signal and the naïve envelope signal, viz.  $SA_q$  and  $SA'_q$  respectively for  $q \in \{1, 2\}$ , are shown to be order optimal for a specific class of  $p$ -times differentiable signals as stated below.*

- (i) *The approximation error of the optimal  $\mathcal{L}_2$  envelope signal,  $SA_2$ , is order optimal to the approximation error of the naïve envelope signal,  $SA'_2$  for the class of  $p$ -times differentiable signals where Fourier coefficients,  $|a_1[k]| = \frac{1}{|k|^p}$  for  $|k| > L$ . That is,*

$$1 \leq \frac{SA'_2}{SA_2} \leq \left(1 + \frac{1}{L}\right)^{2p-1}.$$

- (ii) *The approximation error of the optimal  $\mathcal{L}_1$  envelope signal,  $SA_1$  is the same as the approximation error of the naïve envelope signal,  $SA'_1$  for the class of  $p$ -times differentiable signals with Fourier coefficients,  $a_1[k] \geq 0$  (non-negative) and  $a_1[k] = a_1[-k]$  (symmetric) for all  $k \in \mathbb{Z}$ . That is,*

$$SA_1 = SA'_1 = 2 \sum_{k>L} a_1[k].$$

The detailed proof is shown in [Appendix A](#).

*Remark:* The above result is shown for one (that is  $D = 1$ ) client device. For  $D$  clients with a sum signal analytic at the server (that is  $\widehat{s}(t) := \sum_{i=1}^D \widehat{f}_i(t)$ ),  $SA_1$  as well as  $SA'_1$  scale linearly

with  $D$ . In contrast,  $SA_2$  and  $SA'_2$  will scale quadratically with  $D$ . Thus in both  $\mathcal{L}_1$  and  $\mathcal{L}_2$  norm based error, the ratio between the approximation errors will remain the same, as in the  $D = 1$  case discussed in the proof.

#### 4.3. CDF of the Envelope Signal Approximation

The CDF is a useful signal analytic to determine various statistical functions, especially in a distributed learning setting such as federated learning. Functions of the CDF estimates are beneficial in estimating customer usage statistics such as mean, median or peak demand in the electricity smart metering illustrated in Fig. 1. By invoking Theorem 1, we derive performance bounds on the estimated CDF obtained from the envelope approximation algorithms (see Sec. 3). Let  $F_X(x)$  denote the CDF of the actual signal  $X(t)$  and let  $F_{X_{\text{env}}}(x)$  be the CDF of the envelope signal approximation,  $\widehat{X}_{\text{env}}(t)$ , with  $(2L + 1)$  Fourier coefficients. In the result below, we characterize an upper bound on the pointwise difference between the actual and the estimated CDFs, as stated below.

**Theorem 2.** *The pointwise difference between the CDF of the actual signal,  $F_X(x)$  and the CDF of the envelope signal approximation,  $F_{\widehat{X}_{\text{env}}}(x)$ , with  $(2L + 1)$  Fourier coefficient is bounded by,*

$$F_X(x) - F_{\widehat{X}_{\text{env}}}(x) \leq \frac{C}{L^{\frac{2p-1}{3}}}, \quad (14)$$

where  $C = \left(4^{\frac{1}{3}} + 2 \times 4^{-\frac{2}{3}}\right) \frac{f_{X,\max}^{2/3}}{(2p-1)^{1/3}}$  and  $f_{X,\max} := \max_x \left[ \frac{dF_X(x)}{dx} \right]$ .

The proof of this result is available in [Appendix B](#)

#### 4.4. Effect of Subsampling on CDF estimate

In practice, signals are obtained as discrete samples over a finite interval. Thus, it is essential to understand how envelope approximation can be performed over signal samples and evaluate the tradeoff between the envelope approximation error and the sampling rate. In this connection, we will consider the aspect of signal sampling while limiting the discussion to the  $\mathcal{L}_2$  distortion. However, a similar analysis also extends to the  $\mathcal{L}_1$  distortion metric. The envelope signal approximation problem posed in (7) is reformulated to reflect the finite signal sample assumption as described below. If  $\vec{b}_{\text{opt}}$  represents the minimizer of  $\mathcal{L}_2$  distance metric applied in (7), then we define,

$$\begin{aligned} \vec{b}_{\text{appopt},n} &:= \arg \min_{\vec{b}} \sum_{|k| \leq L} |b[k] - a[k]|^2 + \sum_{|k| > L} |a[k]|^2 \\ &\text{subject to } \widehat{f}_{\text{env}}(t_n) \geq f(t_n), \quad \forall t_n \in \left\{0, \frac{1}{n}, \frac{2}{n}, \dots, 1\right\}, \end{aligned} \quad (15)$$

where  $n$  is a positive integer denoting the number of signal samples. Also, we define the approximately optimal envelope signal,  $f_{\text{appopt},n}(t) := \vec{b}_{\text{appopt},n}\Phi(t)$ . The above formulation in (15) has only finite inequality constraints as against the infinite inequality constraints in (7). Due to the relaxation of the envelope constraints attributed to signal sampling, the  $\mathcal{L}_2$  cost of the approximately optimum envelope is lesser than the optimum envelope. This difference in the  $\mathcal{L}_2$  cost of the envelope error, for the infinite envelope constraint and the sampled envelope constraint relaxation as characterized in [27] is written as,

$$\sum_{|k|\leq L} \left[ |b_{\text{opt}}[k] - a[k]|^2 - |b_{\text{appopt},n}[k] - a[k]|^2 \right] \leq 2(b_{\text{appopt},n}[0] - a[0]) \left( \frac{c + c'}{n} \right) + o(1/n). \quad (16)$$

The constants  $c$  and  $c'$  in the above upperbound expression corresponds to the maximum slopes of the actual signal and the approximately optimal envelope signal respectively. That is,  $|f'(t)| \leq c$  and  $|f'_{\text{appopt},n}(t)| := c'$ . The upperbound on  $c'$  is shown to be  $2\pi L\|f\|_\infty$ , in [27].

Let  $F_X(x)$  be the CDF of the actual signal,  $X(t) := \sum_{k \in \mathbb{Z}} A[k] \exp(j2\pi kt)$  for  $t \in [0, 1]$ . Further, let  $F_{X_{\text{appopt},n}}(x)$  be CDF of the envelope signal approximation with the subsampled constraints,  $\hat{X}_{\text{appopt},n}(t) := \sum_{|k|\leq L} B_{\text{appopt},n}[k] \exp(j2\pi kt)$  for  $t \in [0, 1]$ , where the set of coefficients  $\{B_{\text{appopt},n,i}[k] : -L \leq k \leq L\}$  is as defined in (15). An upperbound between the pointwise difference of the two CDFs is shown below,

**Theorem 3.** *The pointwise difference between the CDF of the actual signal,  $F_X(x)$  and the CDF of the subsampled envelope signal approximation,  $F_{X_{\text{appopt},n}}(x)$ , with  $(2L + 1)$  Fourier coefficient is bounded by,*

$$F_X(x) - F_{X_{\text{appopt},n}}(x) \leq C \times \left\{ \frac{4}{2^p - 1} \frac{1}{L^{2p-1}} + 8\mu_{\text{appopt},n} \frac{c + c'}{n} + o(1/n) \right\}^{1/3}, \quad (17)$$

where  $C = \left(2^{\frac{1}{3}} + 2^{-\frac{2}{3}}\right) f_{X,\max}^{2/3}$  and  $f_{X,\max} := \max_x \left[ \frac{dF_X(x)}{dx} \right]$ . The constant,  $\mu_{\text{appopt},n} = \mathbb{E} [B_{\text{appopt},n}[0] - A[0]]$ , where  $B_{\text{appopt},n}[0]$  and  $A[0]$  are the zero frequency components corresponding to the signals  $\hat{X}_{\text{appopt},n}(t)$  and  $X(t)$  respectively.

The proof of this result is available in [Appendix C](#).

## 5. Experimental Results and Discussion

### 5.1. Electricity Consumption Dataset

To showcase the effect of envelope approximation in a federated learning model, we have performed experiments on an existing electrical energy consumption dataset [11], consisting of hourly energy consumption of 39 users from a residential building. Users with atleast 30 days

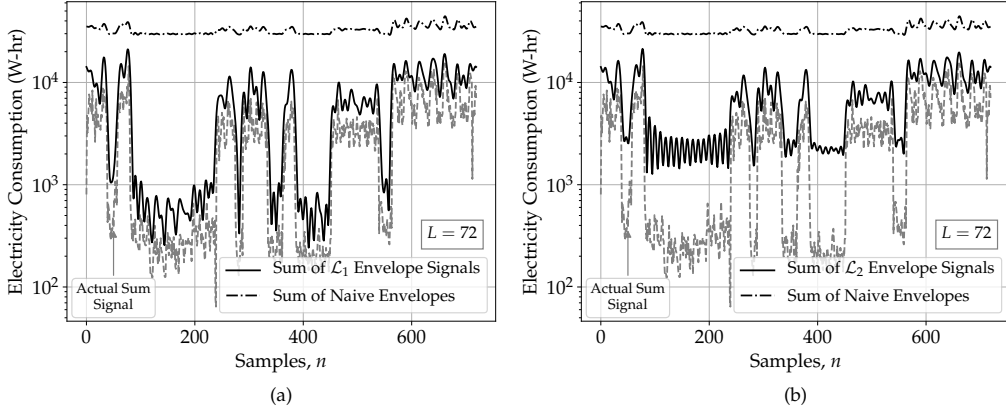


Figure 3: The sum of client signals obtained by distributed envelope approximation schemes are compared with the ground truth signal, when the number of coefficients communicated are  $L = 72$ . Plot (a) and (b) consider  $\mathcal{L}_1$  and  $\mathcal{L}_2$  cost functions respectively. It is observed that the optimal envelope approximation signal estimates the peak energy demand regions.

of synchronized timestamps are filtered for the experiments discussed here – which results in 37 users. In the considered dataset, energy measurements are available in three phases. However, we have restricted to only a single phase, namely W3 in the dataset.

**Hardware/Software Configuration:** The simulations on the dataset were performed in a PC with the Processor model – Intel(R) Core(TM) i3-2310M CPU @ 2.10GHz, 2100 Mhz, 2 Core(s), RAM 6 GB; and implemented in MATLAB 2015b (Windows platform) using the standard curve fitting toolbox and CVX package (ver 2.1).

### 5.2. Tradeoff between Communication Cost and Approximation Error

We analyze the tradeoff between the number of communicated Fourier coefficients and the envelope approximation error by considering a sum signal analytic (or the sum of user energy consumptions, refer 8), which is learned at the central server. Each Fourier coefficient communicated to the server is a real-valued floating point number typically 4 Bytes (or 32 bits). Thus, each client device (i.e., the 37 users) computes the Fourier coefficients of the envelope approximation, which represents 30 days of hourly data, or 720 signal samples (refer Fig. 3(a)-(b) for the time-series plot of the sum signal analytic). Fig. 4 shows the tradeoff plot between the relative root mean-squared (RMS) error and the number of Fourier coefficients. We observe a graceful degradation of the RMS error with respect to the number of coefficients, for the optimal envelope approximation, derived using the  $\mathcal{L}_1$  and  $\mathcal{L}_2$  cost functions. We note that the RMS error in the distributed signal approximation schemes approach zero when 720 Fourier coefficients are transmitted. However, for the considered dataset, the naive approximation fails to capture the envelope trend. In Fig. 4, we have indicated two extremum points – one corre-

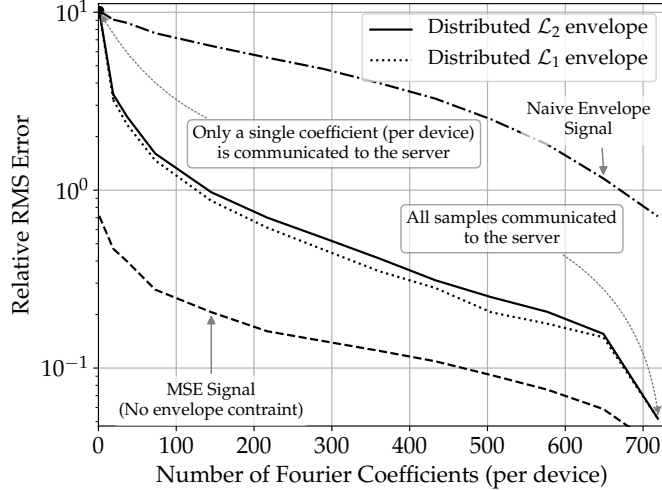


Figure 4: The depiction of the tradeoff between normalized root mean-squared (RMS) error and the number of Fourier coefficients communicated per device. The distributed envelope signal approximation based on  $\mathcal{L}_1$  and  $\mathcal{L}_2$ -norms converge to the zero error with increase in the number of communicated signal coefficients. The plot also shows the RMS error for the naïve envelope signal and the MSE optimal signal (which is devoid of any envelope constraints).

sponding to the least communication scheme (that is  $L = 1$ ), and the other where all coefficients are communicated (that is  $L = 360$ ). The  $\mathcal{L}_1$  cost function results in a relatively lower RMS error compare to  $\mathcal{L}_2$ , which is attributed to the better time-series fit of  $\mathcal{L}_1$  as shown in Fig. 3. Further, it can be observed that the relative approximation error of classical MSE minimizer (that is, without the envelope constraint) is lower than optimal  $\mathcal{L}_1$  and  $\mathcal{L}_2$  distributed envelopes by one order of magnitude.

### 5.3. Signal Analytics based on Cumulative Distribution Function

In this experiment, we study the signal analytics learned from the CDF of the reconstructed envelope signals. At the central server, we compute empirical CDFs using the Glivenko Cantelli estimate, which are later processed to infer statistical properties involving symmetric function. Fig. 5 illustrates the convergence of the estimated CDF (from envelope approximations using the  $\mathcal{L}_2$  cost) to the baseline CDF, which is constituted by all the raw data observed at the clients. For lower approximations, e.g.  $L = 36$ , the CDF estimate performs poorly for the mid-signal ranges ( $x \in [200, 1500]$ ) while being able to accurately track the signal peaks ( $x \in [2000, 4000]$ ). The gap between the estimate and the baseline reduces with an increase in approximation coefficients,  $L$ . We note that the overpredicted CDF always appears towards the right of the true CDF due to the envelope constraint.

Next, we attempt to infer quantile estimates from these CDF plots. In Table 1, we compare the quantiles of the actual CDF with the quantiles of the CDF estimates. We note that  $\mathcal{L}_1$

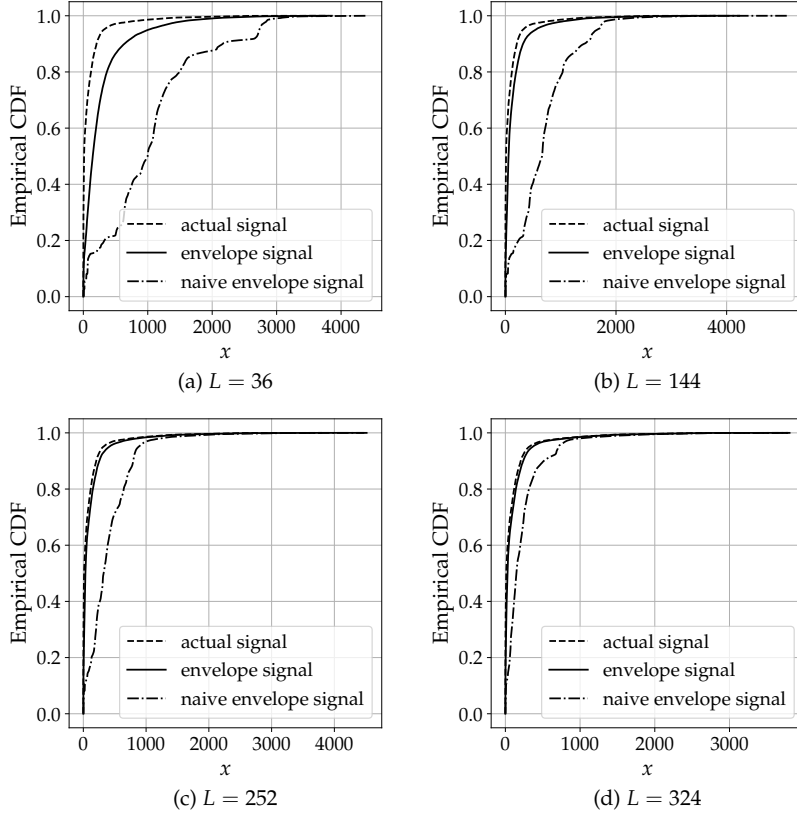


Figure 5: Plot shows the empirical CDF approximation at different approximation levels  $L$  and illustrates its convergence to the actual CDF for the  $\mathcal{L}_2$  cost function. Note that the optimum and the naïve envelope signal CDFs always appear on the right of the actual CDF due to the envelope constraint.

based quantile estimates provide a closer approximation to the actual signal quantile as when compared to  $\mathcal{L}_2$  scheme. Also, the higher-order quantiles deviate much compared to the lower ones, which is attributed to the overprediction constraint at the devices. For comparison, we have also included the quantiles that correspond to the naïve envelope signal. By choosing an appropriate basis representation, we can improve the accuracy of the quantile estimates in Table 1. We shall address this in a future work.

#### 5.4. Effect of Subsampling

In practice, as the signal acquisition in the edge device will not be a recording a continuous signal, we will investigate the effect of signal sampling on the envelope approximation algorithms. Since the dataset considered here is already discrete time-series with 720 samples, we will see the effect of subsampling on the various performance metrics. In particular, for this experimental study we consider three performance error metric, *viz.* (i) Wasserstein distance between the estimated envelope CDF and the actual CDF, (ii) Number of envelope constraint violations with respect to the actual 720 samples, and (iii) Peak envelope error after subsampling. We have used the 1-D Wasserstein distance between the CDF of the envelope signal and the CDF

Table 1: A comparison of the quantiles of the true signal with the envelope approximation signal

Quantile	Actual Signal	Cost Function	Envelope Signal			Naïve Envelope Signal		
			$L = 36$	$L = 180$	$L = 324$	$L = 36$	$L = 180$	$L = 324$
10%	0	$\mathcal{L}_1$	0.21	$10^{-6}$	$10^{-7}$	66.34	39.19	7.79
		$\mathcal{L}_2$	3.39	0.80	0.11			
50%	6.09	$\mathcal{L}_1$	19.25	10.12	6.78	754.85	410.91	116.05
		$\mathcal{L}_2$	65.36	27.55	13.36			
90%	204.53	$\mathcal{L}_1$	429.59	272.41	225.71	2162.7	1229.2	514.11
		$\mathcal{L}_2$	431.21	268.6	218.42			

of the actual signal, that is defined as,

$$\mathcal{W}(X, \hat{X}_{\text{env}}) := \int_0^1 \left| F_X^{-1}(z) - F_{\hat{X}_{\text{env}}}^{-1}(z) \right| dz,$$

where  $F_{\hat{X}_{\text{env}}}(x)$  is the envelope signal CDF and  $F_X(x)$  is the true signal CDF. The number of envelope constraint violations and the peak envelope error are computed based on the pointwise difference between the sum of envelope approximated time-series and the sum of actual time-series. In Fig .6, we show the various performance metrics considering the  $\mathcal{L}_1$  cost function for different subsampling rate, i.e.  $S \in \{1, 2, 4, 8\}$ . At a subsampling rate of  $S$ , the number of envelope constraints is  $720/S$ . From Fig. 6 (a), it is observed that subsampling by considering alternate signal samples, i.e.  $S = 2$ , reduces the Wasserstein distance between the CDFs of the envelope signal and the true signal, when compared with the envelope without subsampling, i.e.  $S = 1$ . This is attributed to the envelope constraint relaxation upon subsampling, which results in a lesser minima for the same objective function. Since the CDF of the MSE approximation signal does account for the envelope constraints the Wasserstein distance approach zero with increasing approximation coefficients, as shown in Fig. 6 (a).

However, subsampling introduces violations of the envelope constraint as shown in Fig. 6 (b)-(c). Both the percentage of envelope constraint violations and the peak error due to envelope constraint violation increase with the number of approximation coefficients  $L$ . This is because of the effect of signal aliasing and signal overfitting introduced due to subsampling. Further it is noted that the signal reconstruction from subsampled time-series fails when the number of Fourier coefficients is more than the total number of signal samples, i.e.  $2L + 1 \geq 720/S$ . In this case envelope approximation algorithm fails to solve the optimization program owing to rank deficiency. This effect is shown in Fig. 6 (a), where the Wasserstein distance returned by

the solver starts to increase at  $L = 45$  for  $S = 8$  and  $L = 90$  for  $S = 4$ . For  $S = 2$ , the rank violation will begin at  $L = 180$  although not shown in the plot.

The rank deficiency also results in an abrupt increase in envelope errors as depicted in Fig. 6 (b)-(c). The tradeoff between the sampling rate, Wasserstein’s distance and the envelope violations, suggests that envelope approximation algorithm should be limited to  $2L+1 < 720/S$ , where the aliasing effects due to subsampling are small. A similar trend is seen to hold when the  $\mathcal{L}_1$  cost function is replaced by the  $\mathcal{L}_2$  cost function. We make a comparison between the envelope approximation algorithms of  $\mathcal{L}_1$  and  $\mathcal{L}_2$  cost functions based on the three performance metrics for  $S = 2$  in Table 2. Due to the relatively poor signal fitting of the  $\mathcal{L}_2$  compared to  $\mathcal{L}_1$  as shown in Fig. 3, the Wasserstein distance is more for  $\mathcal{L}_2$  cost. However the number of envelope errors and the peak envelope error is reduced because of the higher envelope constraint guard region at lower signal amplitudes for the  $\mathcal{L}_2$  approximation. Thus, for the low envelope approximation regime, i.e.  $L = 10$  to  $L = 50$ , it is suggestive to employ the  $\mathcal{L}_2$  approximation algorithm when subsampling, as the envelope constraint violations are better controlled.

Table 2: Comparison of different error metric for the  $\mathcal{L}_1$  and the  $\mathcal{L}_2$  cost functions, assuming  $S = 2$  subsampling

Error Metric	Cost Function	Envelope Approximation							
		$L = 10$	$L = 20$	$L = 30$	$L = 40$	$L = 50$	$L = 60$	$L = 70$	$L = 80$
Wasserstein Distance	$\mathcal{L}_1$	9725.63	6396.24	4775.37	3390.32	2906.97	2370.42	1913.22	1670.10
	$\mathcal{L}_2$	11378.52	8051.19	6050.24	4403.93	3867.93	3220.06	2725.07	2400.25
Number of Envelope Violations	$\mathcal{L}_1$	0	1	0	4	4	6	8	10
	$\mathcal{L}_2$	0	0	0	2	2	5	6	7
Peak Envelope Error (in W-Hr)	$\mathcal{L}_1$	0	408.26	0	1158.47	1484.85	1756.70	2313.55	2581.35
	$\mathcal{L}_2$	0	0	0	683.21	793.70	1271.43	2044.13	2363.26

## 6. Conclusions

In this paper, we proposed signal approximation algorithms to perform overprediction of distributed signals in a client-server federated learning model. Using a convex optimization framework, we determine overpredicting signal representations locally at each edge device, further communicating these to the cloud server to compute signal analytics. Such signal analytics, like the aggregate signal or the Cumulative Distribution Function (CDF) of the time-series signal, derived from the individual signal representations using federated aggregation, were analyzed to determine the tradeoff characteristics between the mean-squared approximation error and

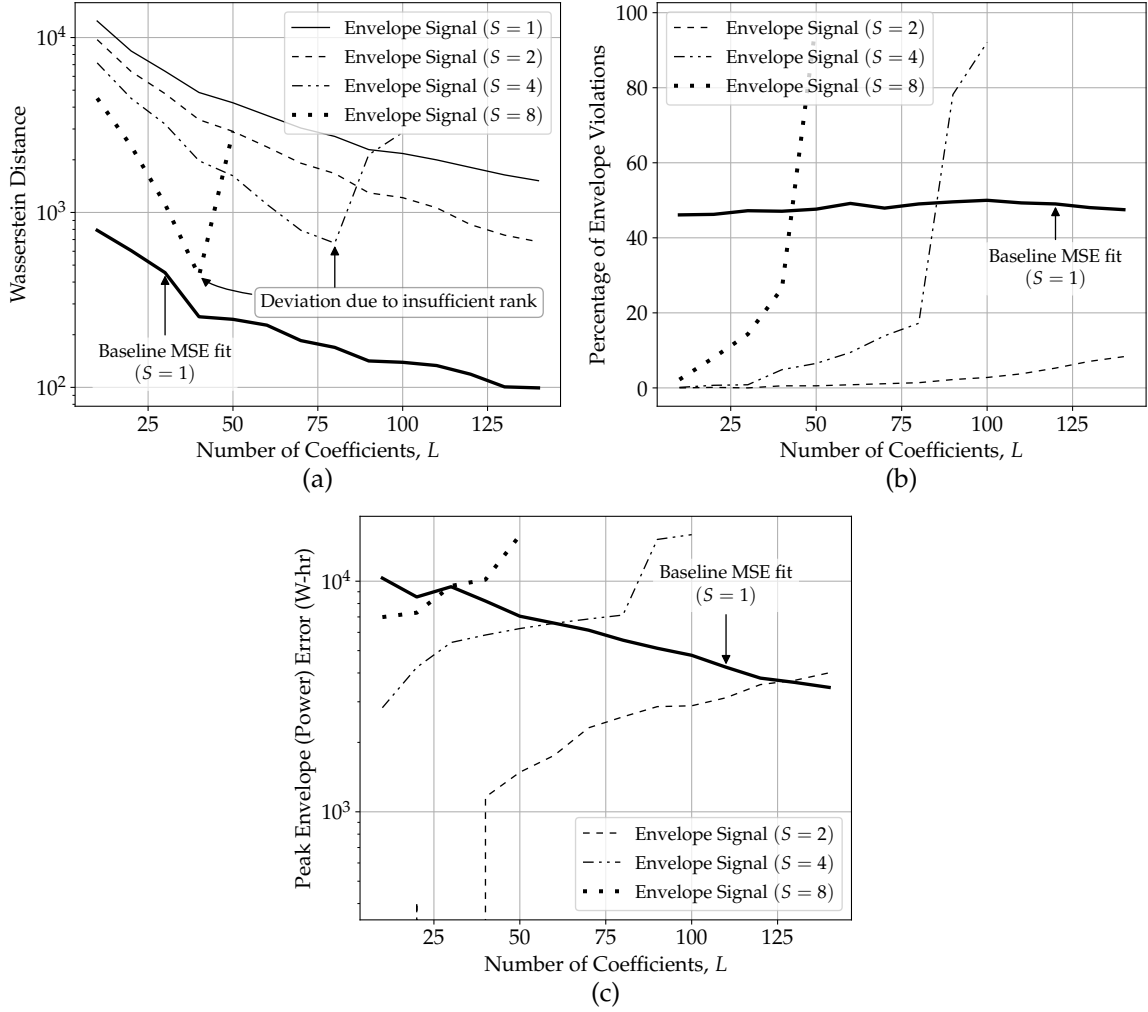


Figure 6: The figures depict the effect of subsampling on the  $\mathcal{L}_1$  cost based envelope approximation based on three performance metrics: (a) Wasserstein distance of estimated envelope CDF and true CDF, (b) percentage of envelope violations at different subsampling rates, (c) peak envelope error due to subsampling.

the number of approximation coefficients (communicated bytes). Particularly for the CDF approximation, we used the Glivenko-Cantelli estimate to estimate upperbounds on the pointwise difference between the actual CDF and the approximate CDF. Experiments on a residential energy consumption dataset validate the analytical performance bounds of the envelope signal analytics considered. In the future, we envisage extending the proposed algorithms for time-series prediction considering the signal overprediction constraints.

## Appendix A. Order Optimality of Envelope Approximation

*Proof.* : We show the desired result for  $q = 2$  and  $q = 1$  separately. For notational simplicity we will consider the following analysis with respect to client device 1 with observed signal being  $f_1(t)$  and the corresponding Fourier coefficients as  $\{a_1[k] : k \in \mathbb{Z}\}$ . The envelope approximation

and its Fourier coefficients are represented as  $\widehat{f}_{1,\text{env}}(t)$  and  $\{b_1[k] : -L \leq k \leq L\}$  respectively.

**Case 1:** For  $q = 2$ , the optimal envelope approximation error is computed from the envelope constraint  $\vec{b}_1^T \Phi(t) \geq f_1(t)$ . Since  $f_1(t) = \sum_{k \in \mathbb{Z}} a_1[k] \exp(j2\pi kt)$  for  $t \in [0, 1]$ , we have the bound

$$\begin{aligned} \sum_{|k| \leq L} b_1[k] \exp(j2\pi kt) &\geq \sum_{k \in \mathbb{Z}} a_1[k] \exp(j2\pi kt) \\ \Rightarrow \sum_{|k| \leq L} (b_1[k] - a_1[k]) \exp(j2\pi kt) &\geq \sum_{|k| > L} a_1[k] \exp(j2\pi kt), \end{aligned}$$

that leads to the inequality  $\sum_{|k| \leq L} |b_1[k] - a_1[k]|^2 \geq \sum_{|k| > L} |a_1[k]|^2$ , based on the Parseval's Theorem. Now, the approximation error of the optimal  $\mathcal{L}_2$ -norm envelope approximation signal,

$$\begin{aligned} \text{SA}_2 &:= \min_{\vec{b}_1} \sum_{|k| \leq L} |b_1[k] - a_1[k]|^2 + \sum_{|k| > L} |a_1[k]|^2 \\ &\geq \min_{\vec{b}_1} 2 \sum_{|k| > L} |a_1[k]|^2. \end{aligned} \quad (\text{A.1})$$

Further, using Fact 1 for  $p$ -times differentiable signal class with  $a_1[k]$ ,  $k \in \mathbb{Z}$  satisfying the lower bound [29] for the series  $\sum_{|k| > L} \frac{1}{|k|^{2p}}$ ,

$$\text{SA}_2 \geq \frac{2}{2p-1} \frac{1}{(L+1)^{2p-1}}. \quad (\text{A.2})$$

Using (13), the approximation error of the naïve envelope can be upper bounded as [29],

$$\text{SA}'_2 \leq \frac{2}{2p-1} \frac{1}{L^{2p-1}}. \quad (\text{A.3})$$

Since  $\text{SA}_2$  refers to the approximation error of the optimal envelope,  $\text{SA}_2 \leq \text{SA}'_2$ , and we get the inequality,

$$1 \leq \frac{\text{SA}'_2}{\text{SA}_2} \leq \left[ \frac{2}{2p-1} \frac{1}{L^{2p-1}} \right] \bigg/ \left[ \frac{2}{2p-1} \frac{1}{(L+1)^{2p-1}} \right], \quad (\text{A.4})$$

or  $1 \leq \frac{\text{SA}'_2}{\text{SA}_2} \leq (1 + \frac{1}{L})^{2p-1}$ . The right hand upperbound approaches 1 in the limit  $L \rightarrow \infty$ . This shows that the approximation errors of the optimal envelope and the naïve envelope are order optimal for the  $\mathcal{L}_2$  cost.

**Case 2:** The optimality of the naïve envelopes for the  $\text{SA}_1$  distance holds for a signal class with the following additional properties:

- (i) the Fourier coefficients  $a_1[k] \geq 0$ ,
- (ii)  $f_1(t)$  is real and even, that is  $a_1[k] = a_1[-k]$ .

From these symmetry assumptions, it follows that  $b_1[k] = b_1[-k]$ . Restricted to this signal class, the  $\text{SA}_1$  envelope approximation is re-stated as:

$$\begin{aligned} \text{SA}_1 &:= \min_{b_1[k], |k| \leq L} b_1[0] - a_1[0], \quad \text{subject to} \\ b_1[0] + 2 \sum_{1 \leq k \leq L} b_1[k] \cos(2\pi kt) &\geq \sum_{k \in \mathbb{Z}} a_1[k] e^{j2\pi kt} \end{aligned} \quad (\text{A.5})$$

The above optimization can be shown to result in  $b_{1,\text{opt}}[0] - a_1[0] = \sum_{|k|>L} a_1[k]$ , using the following argument. Consider the envelope constraint in (A.5), by rearranging the terms,

$$b_1[0] - a_1[0] \geq 2 \sum_{1 \leq k \leq L} (a_1[k] - b_1[k]) \cos(2\pi kt) + 2 \sum_{|k|>L} a_1[k] \cos(2\pi kt). \quad (\text{A.6})$$

Since we assumed  $a_1[k] > 0$  for all  $k$  and  $\{b_1[k] : 1 \leq k \leq L\}$  is the optimization variable, the right hand side term of the above inequality is maximum at  $t = 0$  and  $t = 1$ . Thus, by choosing  $b_1[k] = a_1[k]$  for  $1 \leq k \leq L$ , we get  $\text{SA}_1 := b_{1,\text{opt}}[0] - a_1[0] \geq 2 \sum_{k>L} a[k]$ . For the considered signal class, the naïve approximation error,  $\text{SA}'_1$  is shown to satisfy  $\text{SA}'_1 = C_0 = \|f_1 - f_{1,\text{proj}}\|_\infty \leq 2 \sum_{k>L} a_1[k]$  using (13). Since the optimal envelope has the minimum approximation error,  $\text{SA}_1 \leq \text{SA}'_1$ . In summary,

$$2 \sum_{k>L} a_1[k] \leq \text{SA}_1 \leq \text{SA}'_1 \leq 2 \sum_{k>L} a_1[k], \quad (\text{A.7})$$

which shows that  $\text{SA}_1 = \text{SA}'_1$  for the signal class considered.

*Remark:* From (6), the  $L_\infty$  norm envelope distortion is expressed as an upper bound in terms of the Fourier coefficients. For the  $p$ -times differentiable signal class, this results in a distortion,  $\text{SA}'_\infty = \mathcal{O}\left(\frac{1}{L^{p-1}}\right)$ , on the naïve approximation scheme, as expressed in Table A.3. We observe that an analytical expression for  $\text{SA}_\infty$  is challenging to determine without additional information on the signal class.  $\square$

Table A.3: Bounds on the approximation errors

$\mathcal{L}_q$ norm	$\text{SA}_q$	$\text{SA}'_q$
$q = 1$	$b_1[0] - a_1[0]$	$\sum_{ k >L}  a_1[k] $
$q = 2$	$\frac{2}{2p-1} \frac{1}{(L+1)^{2p-1}}$	$\frac{2}{2p-1} \frac{1}{L^{2p-1}}$
$q = \infty$	—	$\frac{2}{p-1} \frac{1}{L^{p-1}}$

## Appendix B. Communication vs Accuracy Tradeoff in Envelope CDF Estimation

*Proof.* Using the result from Grimmett and Stirzaker [30], for any  $\epsilon > 0$ ;

$$\begin{aligned} F_{X_{\text{env}}}(x) &\geq F_X(x - \epsilon) - \mathbb{P}(X_{\text{env}} - X > \epsilon) \\ \Rightarrow F_X(x) - F_{X_{\text{env}}}(x) &\leq F_X(x) - F_X(x - \epsilon) + \mathbb{P}(X_{\text{env}} - X > \epsilon) \end{aligned} \quad (\text{B.1})$$

In the limit  $\varepsilon \rightarrow 0$ ,

$$F_X(x) - F_{X_{\text{env}}}(x) \leq \varepsilon f_X(x) + \mathbb{P}(X_{\text{env}} - X > \varepsilon) \quad (\text{B.2})$$

Since  $X_{\text{env}}$  is the  $(2L + 1)$  coefficient envelope approximation,

$$\|X - X_{\text{env}}\|_2^2 = \sum_{|k| \leq L} |B_{\text{env}}[k] - A[k]|^2 + \sum_{|k| > L} |A[k]|^2 \quad (\text{B.3})$$

From the envelope constraint,  $X_{\text{env}}(t) \geq X(t)$ , we have

$$\begin{aligned} \sum_{|k| \leq L} B_{\text{env}}[k] e^{j2\pi kt} &\geq \sum_{k \in \mathbb{Z}} A[k] e^{j2\pi kt} \\ \Rightarrow \sum_{|k| \leq L} (B_{\text{env}}[k] - A[k]) e^{j2\pi kt} &\geq \sum_{|k| > L} A[k] e^{j2\pi kt} \\ \Rightarrow \sum_{|k| \leq L} |B_{\text{env}}[k] - A[k]|^2 &\geq \sum_{|k| > L} |A[k]|^2 \end{aligned} \quad (\text{B.4})$$

Applying the above inequality in (B.3),

$$\begin{aligned} \|X_{\text{env}} - X\|^2 &\leq 2 \sum_{|k| \leq L} |B_{\text{env}}[k] - A[k]|^2 \\ &\leq 2 \sum_{|k| \leq L} |B_{\text{naïve}}[k] - A[k]|^2 \\ &\leq \frac{2}{2p-1} \frac{1}{L^{2p-1}} \quad (\text{Ref: [29]}). \end{aligned} \quad (\text{B.5})$$

We now use the Chebyshev's inequality in (B.1), i.e.

$$\begin{aligned} \mathbb{P}(X_{\text{env}} - X > \varepsilon) &\leq \frac{1}{\varepsilon^2} \mathbb{E}(\|X_{\text{env}} - X\|^2) \\ &\leq \frac{1}{\varepsilon^2} \frac{2}{2p-1} \frac{1}{L^{2p-1}} \end{aligned} \quad (\text{B.6})$$

The difference of the CDF's,

$$F_X(x) - F_{X_{\text{env}}}(x) \leq \varepsilon f_X(x) + \frac{2}{\varepsilon^2(2p-1)} \frac{1}{L^{2p-1}}. \quad (\text{B.7})$$

Assuming  $f_X(x) \leq f_{X,\text{max}}$ , we get  $F_X(x) - F_{X_{\text{env}}}(x) \leq \varepsilon f_X(x) + \frac{2}{\varepsilon^2(2p-1)} \frac{1}{L^{2p-1}}$ . On minimizing the right-hand side w.r.t  $\varepsilon$ , we get,

$$F_X(x) - F_{X_{\text{env}}}(x) \leq \left(4^{\frac{1}{3}} + 2 \times 4^{-\frac{2}{3}}\right) \frac{f_{X,\text{max}}^{2/3}}{(2p-1)^{1/3}} \frac{1}{L^{\frac{2p-1}{3}}} \quad (\text{B.8})$$

□

## Appendix C. Effect of Subsampling on the CDF

Consider the following optimization,

$$\begin{aligned} \min_{\widehat{f}_{\text{env}}} \quad & \|f - \widehat{f}_{\text{env}}\|_2^2 \\ \text{subject to} \quad & f_{\text{env}}(t) \geq f(t), \quad t \in [0, 1]. \end{aligned} \quad (\text{C.1})$$

The same optimization can be re-written in terms of the Fourier Coefficients as,

$$\begin{aligned} \vec{B}_{\text{env}} := \arg \min_{\vec{B}} \quad & \|\vec{A} - \vec{B}\|_2^2 \quad \text{subject to} \\ & \vec{B}^T \Phi(t) \geq f(t), \quad t \in [0, 1], \end{aligned} \quad (\text{C.2})$$

where  $\Phi(t)$  denotes the bandlimited Fourier basis with  $(2L + 1)$  basis elements. Suppose, only discrete samples of the signal was available, the optimization problem to solve would be,

$$\begin{aligned} \vec{B}_{\text{appopt},n} := \arg \min_{\vec{B}} \quad & \|\vec{A} - \vec{B}\|_2^2 \quad \text{subject to} \\ & \vec{B} \Phi(t_n) \geq f(t_n) \quad \text{for } t_n \in \left\{0, \frac{1}{n}, \frac{2}{n}, \dots, 1\right\} \end{aligned} \quad (\text{C.3})$$

Since (C.3) has only a subset of constraints compared to (C.2),

$$\|\vec{A} - \vec{B}_{\text{appopt},n}\|_2^2 \leq \|\vec{A} - \vec{B}_{\text{env}}\|_2^2. \quad (\text{C.4})$$

Using the method in [27], we can construct a suboptimal envelope signal with coefficients  $\vec{B}_{\text{subopt}}$

such that  $B_{\text{subopt}}[k] = \begin{cases} B_{\text{appopt},n}[k], & k \neq 0 \\ B_{\text{appopt},n}[0] + \frac{c+c'}{n}, & k = 0 \end{cases}$ , where the constants arise from the assumptions  $|f'(t)| \leq c$  and  $f'_{\text{appopt},n}(t) \leq c'$ , described in (16). Since  $\vec{B}_{\text{subopt}}$  satisfies the envelope constraint in (C.2), we can write

$$\|\vec{A} - \vec{B}_{\text{appopt},n}\|_2^2 \leq \|\vec{A} - \vec{B}_{\text{env}}\|_2^2 \leq \|\vec{A} - \vec{B}_{\text{subopt}}\|_2^2. \quad (\text{C.5})$$

Similar to the earlier case, we wish to find an upperbound on CDF difference, viz. for all  $\varepsilon > 0$

$$\left| F_X(x) - F_{X_{\text{appopt},n}}(x) \right| \leq \varepsilon f_X(x) + \frac{1}{\varepsilon^2} \mathbb{E}(\|X - X_{\text{appopt},n}\|^2). \quad (\text{C.6})$$

Consider,

$$\begin{aligned}
\|X - X_{\text{appopt},n}\|^2 &\leq \|X - X_{\text{env}}\|^2 + \|X_{\text{env}} - X_{\text{appopt},n}\|^2 \quad (\text{Traingle Inequality}) \\
&= \sum_{|k|\leq L} |B_{\text{env}}[k] - A[k]|^2 + \sum_{|k|\leq L} |A[k]|^2 + \sum_{|k|\leq L} |B_{\text{env}}[k] - B_{\text{appopt},n}[k]|^2 \\
&\leq 3 \sum_{|k|\leq L} |B_{\text{env}}[k] - A[k]|^2 + \sum_{|k|\leq L} |B_{\text{appopt},n}[k] - A[k]|^2 \\
&\leq 4 \sum_{|k|\leq L} |B_{\text{subopt}}[k] - A[k]|^2 \\
&\leq 4 \sum_{|k|\leq L} |B_{\text{appopt},n}[k] - A[k]|^2 + 8(B_{\text{appopt},n}[0] - A[0])\frac{c+c'}{n} + o(1/n) \\
&\leq \frac{4}{2p-1} \frac{1}{L^{2p-1}} + 8(B_{\text{appopt},n}[0] - A[0])\frac{c+c'}{n} + o(1/n) \tag{C.7}
\end{aligned}$$

Thus,

$$\left| F_X(x) - F_{X_{\text{appopt},n}}(x) \right| \leq \varepsilon f_X(x) + \frac{1}{\varepsilon^2} \left\{ \frac{4}{2p-1} \frac{1}{L^{2p-1}} + 8\mu_{\text{appopt},n} \frac{c+c'}{n} + o(1/n) \right\}, \tag{C.8}$$

where  $\mu_{\text{appopt},n} = \mathbb{E}(B_{\text{appopt},n}[0] - A[0])$ . On assuming  $f_X(x) \leq f_{X,\max}$  and minimizing the upper bound with respect to  $\varepsilon$ , we get

$$\left| F_X(x) - F_{X_{\text{appopt},n}}(x) \right| \leq \left[ \left( 2^{\frac{1}{3}} + 2^{-\frac{2}{3}} \right) f_{X,\max}^{2/3} \right] \left\{ \frac{4}{2p-1} \frac{1}{L^{2p-1}} + 8\mu_{\text{appopt},n} \frac{c+c'}{n} + o(1/n) \right\}^{1/3}. \tag{C.9}$$

## References

- [1] L. Sankar, S. R. Rajagopalan, S. Mohajer, H. V. Poor, Smart meter privacy: A theoretical framework, *IEEE Transactions on Smart Grid* Vol: 4 (2) (2013) 837–846. doi:10.1109/TSG.2012.2211046.  
URL <https://doi.org/10.1109/TSG.2012.2211046>
- [2] B. McMahan, E. Moore, D. Ramage, S. Hampson, B. A. y Arcas, Communication-efficient learning of deep networks from decentralized data, in: A. Singh, X. J. Zhu (Eds.), *Proceedings of the 20th International Conference on Artificial Intelligence and Statistics*, Vol. 54 of *Proceedings of Machine Learning Research*, PMLR, 2017, pp. 1273–1282.  
URL <http://proceedings.mlr.press/v54/mcmahan17a.html>
- [3] J. Konečný, H. B. McMahan, F. X. Yu, P. Richtárik, A. T. Suresh, D. Bacon, Federated learning: Strategies for improving communication efficiency, in: *NIPS Workshop*, 2016, p. 1.  
URL <https://arxiv.org/abs/1610.05492>
- [4] J. Konečný, H. B. McMahan, D. Ramage, P. Richtárik, Federated optimization: Distributed machine learning for on-device intelligence, *CoRR* abs/1610.02527 (2016) 1. arXiv:1610.02527.  
URL <http://arxiv.org/abs/1610.02527>
- [5] K. Bonawitz, H. Eichner, W. Grieskamp, D. Huba, A. Ingerman, V. Ivanov, C. Kiddon, J. Konečný, S. Mazzocchi, H. B. McMahan, T. V. Overveldt, D. Petrou, D. Ramage, J. Roslander, Towards federated learning at scale: System design, *CoRR* abs/1902.01046 (2019). arXiv:1902.01046.  
URL <http://arxiv.org/abs/1902.01046>

- [6] P. Kairouz, H. B. McMahan, Advances and open problems in federated learning, *Foundations and Trends in Machine Learning* 14 (1) (2021) –. doi:10.1561/22000000083.  
URL <http://dx.doi.org/10.1561/22000000083>
- [7] T. Li, A. K. Sahu, A. Talwalkar, V. Smith, Federated learning: Challenges, methods, and future directions, *IEEE Signal Processing Magazine* 37 (3) (2020) 50–60. doi:10.1109/MSP.2020.2975749.  
URL <https://doi.org/10.1109/MSP.2020.2975749>
- [8] A. T. Suresh, F. X. Yu, S. Kumar, H. B. McMahan, Distributed mean estimation with limited communication, in: *Proceedings of the 34th International Conference on Machine Learning, ICML 2017, Sydney, NSW, Australia, 6-11 August 2017*, Vol. 70 of *Proceedings of Machine Learning Research*, PMLR, 2017, pp. 3329–3337.  
URL <http://proceedings.mlr.press/v70/suresh17a.html>
- [9] M. M. Amiri, D. Gündüz, Federated learning over wireless fading channels, *IEEE Transactions on Wireless Communications* 19 (5) (2020) 3546–3557. doi:10.1109/TWC.2020.2974748.  
URL <https://doi.org/10.1109/TWC.2020.2974748>
- [10] Google AI Blog federated analytics: Collaborative data science without data collection, <https://ai.googleblog.com/2020/05/federated-analytics-collaborative-data.html>, accessed: 2021-05-19 (2020).
- [11] P. M. Mammen, H. Kumar, K. Ramamritham, H. Rashid, Want to reduce energy consumption, whom should we call?, in: H. Schmeck, V. Hagenmeyer (Eds.), *Proceedings of the Ninth International Conference on Future Energy Systems, e-Energy 2018, Karlsruhe, Germany, June 12-15, 2018*, ACM, 2018, pp. 12–20. doi:10.1145/3208903.3208941.  
URL <https://doi.org/10.1145/3208903.3208941>
- [12] A. Nilsson, S. Smith, G. Ulm, E. Gustavsson, M. Jirstrand, A performance evaluation of federated learning algorithms, in: *Proceedings of the Second Workshop on Distributed Infrastructures for Deep Learning, DIDL@Middleware 2018, Rennes, France, December 10, 2018*, ACM, 2018, pp. 1–8. doi:10.1145/3286490.3286559.  
URL <https://doi.org/10.1145/3286490.3286559>
- [13] D. Alistarh, D. Grubic, J. Li, R. Tomioka, M. Vojnovic, QSGD: communication-efficient SGD via gradient quantization and encoding, in: *Advances in Neural Information Processing Systems*, 2017, pp. 1709–1720.  
URL <https://proceedings.neurips.cc/paper/2017/hash/6c340f25839e6acdc73414517203f5f0-Abstract.html>
- [14] A. Feraudo, P. Yadav, V. Safronov, D. A. Popescu, R. Mortier, S. Wang, P. Bellavista, J. Crowcroft, Colearn: Enabling federated learning in mud-compliant iot edge networks, in: *Proceedings of the Third ACM International Workshop on Edge Systems, Analytics and Networking*, 2020, pp. 25–30.
- [15] T. Li, M. Sanjabi, A. Beirami, V. Smith, Fair resource allocation in federated learning, in: *8th International Conference on Learning Representations, ICLR 2020, Addis Ababa, Ethiopia, April 26-30, 2020*, OpenReview.net, 2020, p. 1.  
URL <https://openreview.net/forum?id=ByexElsYDr>
- [16] M. Mohri, G. Sivek, A. T. Suresh, Agnostic federated learning, in: K. Chaudhuri, R. Salakhutdinov (Eds.), *Proceedings of the 36th International Conference on Machine Learning*, Vol. 97 of *Proceedings of Machine Learning Research*, PMLR, 2019, pp. 4615–4625.  
URL <http://proceedings.mlr.press/v97/mohri19a.html>
- [17] V. Smith, C. Chiang, M. Sanjabi, A. S. Talwalkar, Federated Multi-Task Learning, in: *Advances in Neural Information Processing Systems*, 2017, pp. 4424–4434.  
URL <https://proceedings.neurips.cc/paper/2017/hash/6211080fa89981f66b1a0c9d55c61d0f-Abstract.html>
- [18] E. White, Statistical learning for unimpaired flow prediction in ungauged basins, Ph.D. thesis, University of California, Davis (2020).

- [19] M. Stockman, M. Awad, R. Khanna, Asymmetrical and lower bounded support vector regression for power estimation, in: 2011 International Conference on Energy Aware Computing, 2011, pp. 1–6. doi:10.1109/ICEAC.2011.6403624.
- [20] T. Van Dijk, G. De Croon, How do neural networks see depth in single images?, in: 2019 IEEE/CVF International Conference on Computer Vision (ICCV), 2019, pp. 2183–2191. doi:10.1109/ICCV.2019.00227.
- [21] G. Maheshwari, A. Kumar, Optimal quantization of tv white space regions for a broadcast based geolocation database, in: 2016 24th European Signal Processing Conference (EUSIPCO), 2016, pp. 418–422. doi:10.1109/EUSIPCO.2016.7760282.
- [22] Y. L. Tun, K. Thar, C. M. Thwal, C. S. Hong, Federated learning based energy demand prediction with clustered aggregation, in: 2021 IEEE International Conference on Big Data and Smart Computing (BigComp), 2021, pp. 164–167. doi:10.1109/BigComp51126.2021.00039.
- [23] K. Bountrogiannis, G. Tzagkarakis, P. Tsakalides, Data-driven kernel-based probabilistic sax for time series dimensionality reduction, in: 2020 28th European Signal Processing Conference (EUSIPCO), 2021, pp. 2343–2347. doi:10.23919/Eusipco47968.2020.9287311.
- [24] Y. M. Saputra, D. T. Hoang, D. N. Nguyen, E. Dutkiewicz, M. D. Mueck, S. Srikanteswara, Energy demand prediction with federated learning for electric vehicle networks, arXiv:1909.00907 (2019).
- [25] V. Anavangot, A. Kumar, Algorithms for overpredictive signal analytics in federated learning, in: 2020 28th European Signal Processing Conference (EUSIPCO), 2021, pp. 1502–1506. doi:10.23919/Eusipco47968.2020.9287390.
- [26] S. Mallat, A Wavelet Tour of Signal Processing, Third Edition: The Sparse Way, 3rd Edition, Academic Press, 2008.
- [27] A. Kumar, Optimal envelope approximation in fourier basis with applications in TV white space, arXiv:1706.00900 (2017).
- [28] M. J. Wainwright, High-dimensional statistics: A non-asymptotic viewpoint, Vol. 48, Cambridge University Press, 2019.
- [29] R. Bhatia, Fourier Series, 2nd Edition, Hindustan Book Agency, 1993.
- [30] G. Grimmett, D. Stirzaker, Probability and Random Processes, Vol. 80, Oxford university press, 2001.